XLIII CILAMCE
21–25, November, 2022
FOZ DO IGUAÇU – PR – BRAZIL

Identification of horizons in seismics using convolutional neural network

Mayara G. Silva[1], Felipe Jordão P. de Andrade[1], Nelia C. Reis1, Marcelo Gattass1

[1]*Tecgraf Institute, Pontifical Catholic University of Rio de Janeiro - PUC-Rio*
Prédio Pe. Laércio Dias de Moura - R. Marquês de São Vicente, 22451-900, Gávea, Rio de Janeiro - RJ, Brazil
mayaragomes@tecgraf.puc-rio.br, felipejordao@tecgraf.puc-rio.br, neliareis@tecgraf.puc-rio.br,
mgattass@tecgraf.puc-rio.br

Abstract. Seismic structural interpretation is an essential step in exploring and producing hydrocarbon reserves. This interpretation requires identifying geological features such as facies, horizons, and faults in the region of interest. The manual identification of these features is a time-consuming task. Convolutional neural networks (CNN) are widely used in computer vision problems, yielding excellent results in many situations, including the seismic interpretation process. This work studies supervised convolutional neural networks to segment horizon lines delimiting seismic facies based on seismic amplitude. We evaluate our proposal using the F3 block with the seismic facie annotations. In the original dataset annotations, the labels were annotated areas for each seismic facies, so this set of annotations was changed from a multiclass problem to a binary, considering only the boundary between one seismic facie to its neighbor. The horizon prediction uses the ResUnet network, a combination of Unet with residual blocks, designed to obtain high performance with fewer parameters. Some loss functions are analyzed to optimize the segmentation result. Generalized dice loss and Focal Tversky loss functions yield best results in our experiments. The Dice metric reached an index above 50% with the Focal Tversky loss function, showing promising results.

Keywords: Data Block F3, Horizon Segmentation, Deep Neural Networks.

1 Introduction

Reservoir characterization is an essential step in the design, development, and production of hydrocarbon reserves. When available, the interpretation is done from a seismic volume of the region of interest. In the interpretation of these data, several characteristics of the geological region are identified, such as the classification of seismic facies, location of horizons, seismic faults, and identification of areas with salt or gas.

Due to a large amount of data, interpreting seismic data performed in a conventional way by an expert is a time-consuming. For this reason, in recent years different methods have been developed to help the geophysics in interpreting, many of those use deep learning solutions.

Deep learning with convolutional neural networks in computer vision problems has evolved a lot nowadays, reaching better results in many problems in this area. Deep learning, unlike traditional classification algorithms used to classify images, does not need the feature extraction step, as the features are learned automatically from the raw data, so it is expected that this technique will be much more successful because it needs less manual engineering [1].

Thus, to help interpreters in the seismic interpretation task, many researchers in the field have invested in methods that use neural networks. Much of the seismic interpretation work using deep learning methods are based on convolutional neural network architectures, but more recent work has invested in recurrent networks. In the seismic facies interpretation task, the authors Zhao [2] and Li et al. [3] present methods using respectively a CNN model based on encoder-decoder, and a model based on attention maps. Alaudah et al. [4] used a VGG16 architecture for the classification of seismic facies, in addition to providing an annotated dataset, obtained from the F3 block. In the identification of horizons (boundaries between seismic facies), Lima [5] presented a deep neural network, the DNFS, based on U-net and StNet, to segment the boundaries. Calhes et al. [6] also propose border detection, where they evaluate the PSP-Net and Deeplab V3+ networks, where they initially identify the seismic facies using a neural network and then detect the borders between them by contour detection. Using a recurrent network, the authors Trinidad et al. [7] applied a neural network in the classification of seismic facies, considering that the seismic data contains temporal information along the axis (inline and crossline), the authors proposed to

use this information in a recurrent neural network, the LSTM, along with other architectures, U-net and Atrous.

So far, different works have been developed in order to assist seismic interpretation tasks. However, many in the field of research, as well as in deep learning, many configurations can still be evaluated. The present work aims to use a convolutional neural network in the supervised mapping of seismic horizons. This work is divided into five sections: Section 2 presents the architecture used to train our models; Section 3 and the annotation used to derive the horizons locations. Then, Section 4 explains the experiments performed, the training parameters, the sample's pre-processing step, and discussion of the results. Finally, Section 5 presents the conclusions.

2 Deep Network Architecture

This section presents a brief description of the techniques used in this work.

2.1 ResUnet

ResUnet is based on U-net and residual learning [8]. U-Net concatenates feature maps from different levels to improve segmentation accuracy [9],and the deep residual learning framework utilizes an identity mapping to facilitate training [10]. Based on these techniques, the deep residual U-Net was proposed, a network with fewer parameters,and can achieve better segmentation results than the U-net.

ResUnet is made up of three parts: the encoding that defines the images in a more compact representation; the bridge serves as a connection between the encoder and decoder; and the decoding that recovers the representations of the images with the segmentation.

2.2 Loss Functions

Deep learning segmentation structures depend not only on the choice of network architecture but also on the choice of a loss function. To define the loss functions used, the ones that best fit segmentation problems were considered. And observing the imbalance between the classes, loss functions that consider this imbalance were also analyzed. Therefore, the functions evaluated were Generalized Dice Loss and Focal Tversky Loss.

Generalized Dice Loss

When the segmentation process targets rare observations, a severe class imbalance between candidate labels is likely to occur, resulting in suboptimal performance. To mitigate this problem, strategies such as the Generalized Dice Loss (GDL) have been proposed [11], which was proposed as a way to evaluate the segmentation of multiple classes with a single score. This function presents a generalized framework for overlays that achieves these goals by defining partial volume and multi-label overlay measures with an associated error measure.

Focal Tversky Loss

The focal Tversky Loss (FTL) function is a combination of the Focal and Tversky functions. The focal loss [12] aims to deal with class disequilibrium. It is based on cross-entropy, using a modulating exponent to reduce weight errors assigned to well-ranked examples, thus preventing a large number of easy negative examples from dominating the gradient to alleviate class disequilibrium. However, it has difficulty balancing precision and recall in small regions of interest. The Tversky function [13] is a Dice score generalization similarity index that allows flexibility in balancing false positives and false negatives.

In the FTL function, if a pixel is misclassified with a high Tversky index, the FTL will not be affected, and if the Tversky index is small and the pixel is misclassified, the FTL will decrease. [14]

3 Seismic Dataset

The dataset used was the Facies-Mark [4], an annotation of geological layers in F3, composed of interval characteristics data and class annotations. The authors defined six classes in these annotations, where each one represents a facies, except one that is the union of two facies, the Rijnland and Chalk. The volume of this data is composed of inline (direction of seismic lines) and crossline (direction perpendicular to seismic lines), and these data are divided into three datasets, training, test 1, and test 2, each having respectively 401, 200 and 601 inline and 701, 701 and 200 crossline.

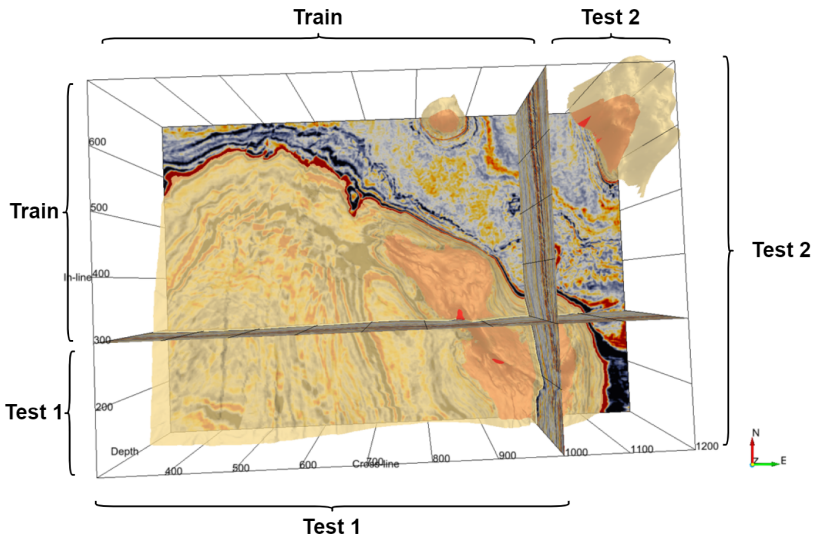

Figure 1. Splitting of the data into training and test set

Figure 1 shows how the 3D model of block F3 was divided into training, test 1, and test 2 sets.

3.1 Preparation of labels

The data of this dataset are annotated considering a multiclass problem, and in this work, considering the problem as binary, it was necessary to adapt the annotations of labels. The objective of this work is to find the edges from one facies to the other since the annotation was defined considering two classes, the background, and the edge. To define a pixel as a horizon, the pixels of the edges of the two facies were considered, considering the horizons with a height of 2. Thus, we would have more information about the characteristics of the transition, which could help in learning this transition.

Figure 2 shows an example of how horizons are defined. Given a multiclass image with facies labels, the pixels on the boundary between two facies are found, then these are defined as horizons with labels 1 and the others are considered background with label 0.

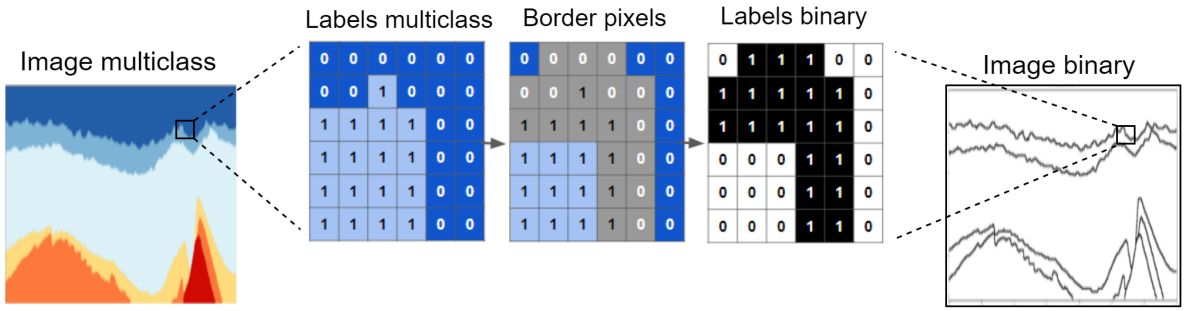

Figure 2. Ground truth labels adapatation.

4 Experiments and Discussion

This section briefly describes the steps of the methodology, the experiments performed and the results obtained.

The method is divided into two stages: pre-processing and segmentation. Figure 3 shows the stages of the methodology.

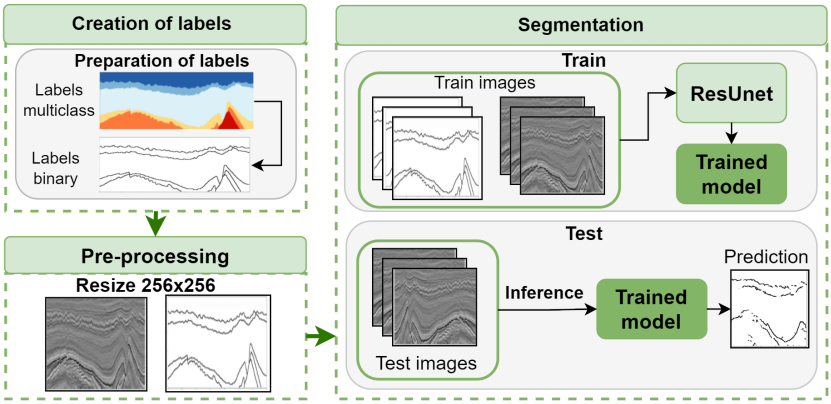

Figure 3. Method steps flowchart

4.1 Pre-processing

The pre-processing step aimed to prepare the images by resizing them for entry into the network. Before this step, the image labels were adapted from multiclass to binary. In this work, all the sets of the dataset were used. The data volume was manipulated in the section format, that is, 2D image, using inlines and crosslines.

Initially, the images were resized to 256x256 to standardize the size of all of them for the neural network input. The data in the dataset is already normalized between -1 and 1, so no further normalization was needed.

4.2 Segmentation

In this stage, the segmentation of horizons and validation of the learning of the models is carried out. First, CNN and loss functions were chosen. Then, the training and inference of the models were performed.

The training set has 1102 images, with dimensions of 255 x 401 for inline and 255 x 701 for crossline. After processing the data, 10% of the training was randomly reserved for the validation set. Then, the amplitude images and the labels of these two sets are passed as input to the neural network for the training phase, which aims to learn the pixels that represent the boundaries.

After the network model is trained, this model is evaluated using the two test sets. After segmenting the test base images, the predicted data are validated with the defined metrics.

4.3 Evaluation Metrics

Metrics aim to measure the method's performance and promote the validation of the results obtained, making it possible to compare and identify the best model configuration for the problem. To evaluate segmentation problems there are some metrics used in the literature. The following metrics were chosen to assess the methodology proposed in this work: Jaccard, Dice, and Recall.

The recall is the number of images correctly classified for the class of interest. The Jaccard index is the calculation of the intersection (overlap) between the set of samples from the manual segmentation with the predicted segmentation on the union between these sets. This metric ranges from 0 to 1, the closer to 1, the greater the intersection between the objects. The Dice coefficient is correlated with Jaccard, it also varies from 0 to 1, the closer to 1, the more similar the predicted segmentation is to the real one. These measurements have the following relationships:

$$Recall = \frac{TP}{TP + FN} \tag{1}$$

$$jaccard(G, P) = \frac{|G \cap P|}{|G \cup P|} = \frac{|G \cap P|}{|G| + |P| - |G \cap P|} \tag{2}$$

$$Dice(G, P) = \frac{2\,|G \cap P|}{|G| + |P|} \tag{3}$$

where horizon, TP is the samples of as horizon; FN is the horizon and non-horizon horizon views); G is the ground truth; and P is the labels predicted by the model.

4.4 Results

All models were implemented using the TensorFlow framework for different loss function configurations. They were trained using the Adam optimizer [15], with a learning rate of 0.001, and training is stopped if there is no improvement in 10 epochs (early stop).

The inference was performed in the inline and crossline sections. The metrics used were Jaccard, Dice, Recall, and standard deviation.

Table 1. Coefficients in constitutive relations

Modelo	Função de perda	Dice (%)	Jaccard (%)	Recall(%)
ResUnet	Generalized Dice	50.48 ± 0.57	34.47 ± 0.49	44.94 ± 1.5
ResUnet	Focal Tversky	51.40 ± 0.51	35.24 ± 0.23	48.02 ± 0.85

Table 1 presents the results obtained. Comparing the values of the metrics, the value functions did not have a significant difference, but both showed promising results, being the Focal Tversky Loss function the one that obtained values a little higher than the Genelarized dice loss, with Dice above 50%, Jaccard of 35%, and Recall of 48%. This function was proposed to identify small ROIs and allows flexibility in the weighting of false positives and false negatives. In the Figures 4, 5, 6, and 7 we can better analyze the results of the metrics by viewing examples of some predictions. In (d) of each image, the overlap between Ground truth and Prediction can be observed.

The problem of finding the boundaries is not trivial, in Figures 4 and 5 we have the result of the prediction of the same section using different loss functions. We can observe in the superposition of both Figures that visually the models obtained good results, managing to identify the borders, missing only the distance of some predicted pixels (blue - errors) from the real labels (green - Ground truth). However, as the metrics are calculated pixel by pixel, the difference in this distance from the predicted pixels to the actual labels affects the results of the metrics, thus obtaining lower values. So, considering this scenario, the results are promising.

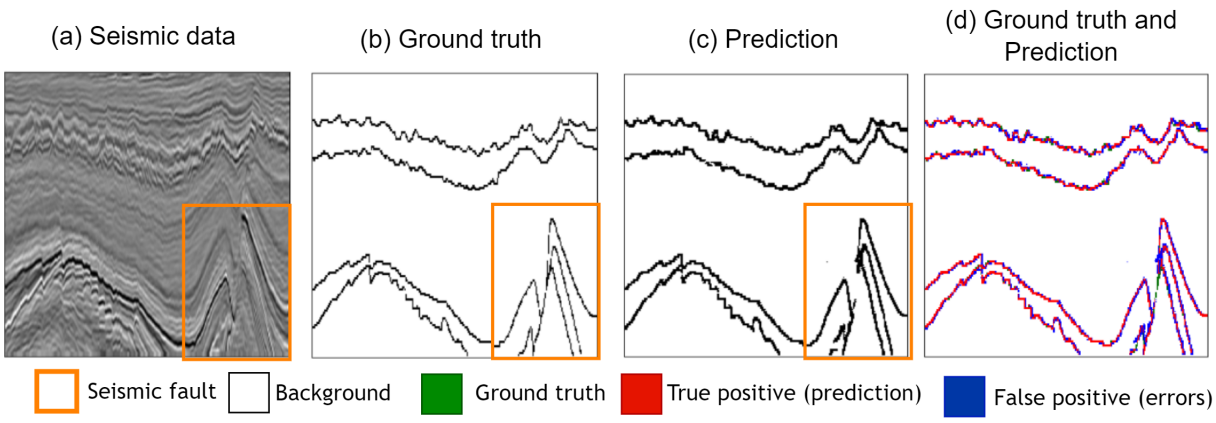

Figure 4. ResUnet forecast result example with Focal Tversky. Dice: 69.59%; Jaccard: 53.36%

Figures 6 and 7 show the same scenario, the result of the prediction of a section using different loss functions. However, unlike the previous images in the overlay, the error of some predicted pixels from the real labels was more visible. The second observation of these examples is the seismic faults that can occur during the acquisition

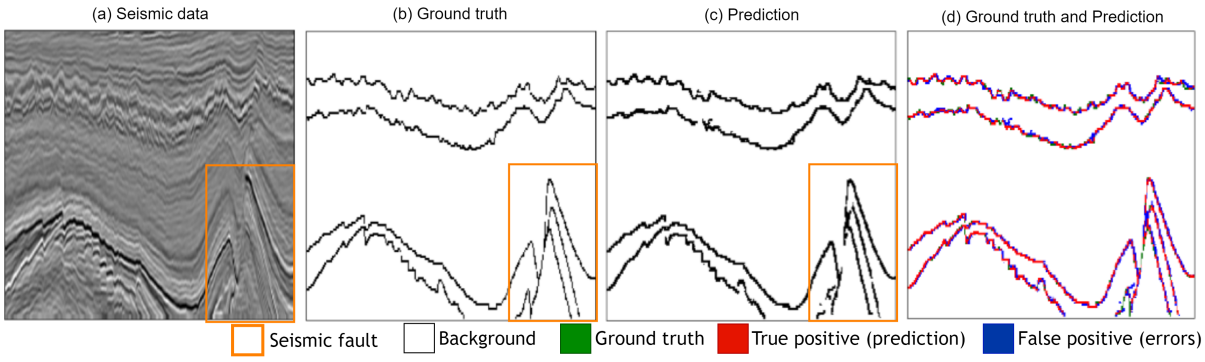

Figure 5. ResUnet forecast result example with Generalized Dice. Index: 69.86%; Jaccard: 53.68%

of these data. In the orange rectangle, it shows an example of a seismic fault, and at that same point the models did not identify this area as a horizon, so it is possible that these faults had a negative influence during the learning of the network, and consequently on the metrics.

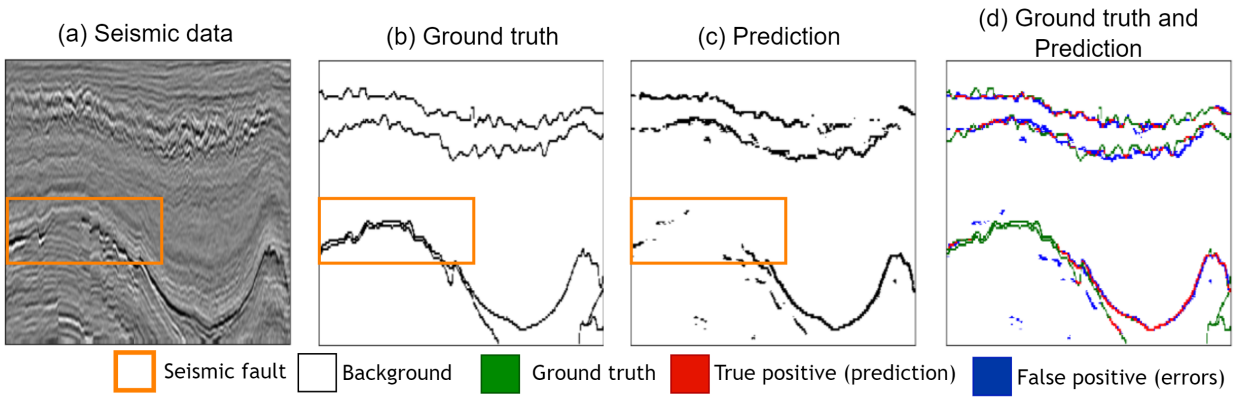

Figure 6. ResUnet forecast result example with Focal Tversky. Dice: 39.82%; Jaccard: 24.86%

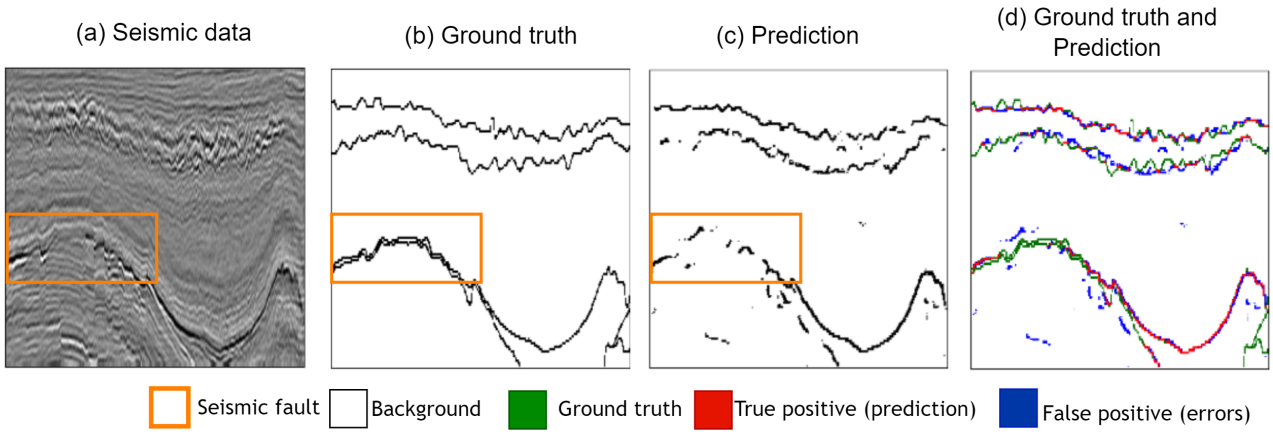

Figure 7. ResUnet forecast result example with Generalized Dice. Dice: 40.28%; Jaccard: 25.22%

5 Conclusions

In this work, the ResUnet neural network was applied by varying the loss function to observe its performance in the binary segmentation of seismic images for the classification of horizons. The results showed that the modeling joining ResUnet and the Focal Tversky Loss function achieved promising results, with Recall of 48% and Dice above 50%.

It was observed that seismic faults negatively influenced the identification of horizons, the model in both loss functions could not identify discontinuities of horizons when there was a fault interval.

After applying and studying ResUnet with different loss functions, we can say that it is a promising technique for the identification of horizons. And there is still a wide variety and configurations of deep learning techniques that can help build a better model where the configurations used in this work did not perform well.

Acknowledgements. The authors are grateful for the support of the Coordination of Superior Level Staff Improvement (CAPES) in the development of this study, granting research funding, and Tecgraf Institute (PUC-Rio).

Authorship statement. The authors hereby confirm that they are the sole liable persons responsible for the authorship of this work, and that all material that has been herein included as part of the present paper is either the property (and authorship) of the authors, or has the permission of the owners to be included here.

References

[1] A. d. S. Ferreira. Redes neurais convolucionais profundas na detecçao de plantas daninhas em lavoura de soja, 2017.

[2] T. Zhao. Seismic facies classification using different deep convolutional neural networks. In *SEG Technical Program Expanded Abstracts 2018*, pp. 2046–2050. Society of Exploration Geophysicists, 2018.

[3] F. Li, H. Zhou, Z. Wang, and X. Wu. Addcnn: An attention-based deep dilated convolutional neural network for seismic facies analysis with interpretable spatial–spectral maps. *IEEE Transactions on Geoscience and Remote Sensing*, vol. 59, n. 2, pp. 1733–1744, 2020.

[4] Y. Alaudah, P. Michałowicz, M. Alfarraj, and G. AlRegib. A machine-learning benchmark for facies classification. *Interpretation*, vol. 7, n. 3, pp. SE175–SE187, 2019.

[5] G. C. Lima. Segmentação de fácies sísmicas com redes neurais, 2021.

[6] D. Calhes, F. K. Kobayashi, A. B. Mattos, M. M. Macedo, and D. A. Oliveira. Simplifying horizon picking using single-class semantic segmentation networks. In *2021 34th SIBGRAPI Conference on Graphics, Patterns and Images (SIBGRAPI)*, pp. 286–292. IEEE, 2021.

[7] M. J. C. Trinidad, S. W. A. Canchumuni, R. Q. Feitosa, and others. Seismic facies segmentation using atrous convolutional-lstm network, 2021.

[8] Z. Zhang, Q. Liu, and Y. Wang. Road extraction by deep residual u-net. *IEEE Geoscience and Remote Sensing Letters*, vol. 15, n. 5, pp. 749–753, 2018.

[9] O. Ronneberger, P. Fischer, and T. Brox. U-net: Convolutional networks for biomedical image segmentation. In *International Conference on Medical image computing and computer-assisted intervention*, pp. 234–241. Springer, 2015.

[10] K. He, X. Zhang, S. Ren, and J. Sun. Deep residual learning for image recognition. In *Proceedings of the IEEE conference on computer vision and pattern recognition*, pp. 770–778, 2016.

[11] W. R. Crum, O. Camara, and D. L. Hill. Generalized overlap measures for evaluation and validation in medical image analysis. *IEEE transactions on medical imaging*, vol. 25, n. 11, pp. 1451–1461, 2006.

[12] T.-Y. Lin, P. Goyal, R. Girshick, K. He, and P. Dollár. Focal loss for dense object detection. In *Proceedings of the IEEE international conference on computer vision*, pp. 2980–2988, 2017.

[13] S. R. Hashemi, S. S. M. Salehi, D. Erdogmus, S. P. Prabhu, S. K. Warfield, and A. Gholipour. Tversky as a loss function for highly unbalanced image segmentation using 3d fully convolutional deep networks. *arXiv preprint arXiv:1803.11078*, 2018.

[14] N. Abraham and N. M. Khan. A novel focal tversky loss function with improved attention u-net for lesion segmentation. In *2019 IEEE 16th international symposium on biomedical imaging (ISBI 2019)*, pp. 683–687. IEEE, 2019.

[15] D. P. Kingma. &ba j.(2014). adam: A method for stochastic optimization. *arXiv preprint arXiv:1412.6980*, 2015.